Hindawi
Geofluids
Volume 2022, Article ID 3166065, 12 pages
https://doi.org/10.1155/2022/3166065

Research Article

Roadway Deformation and Control under Multidisturbed Secondary High Stress

Xiaoguang Sun,[1] Haibin Wang,[2] Xiaofang Wo,[3,4] Zhimeng Sun,[5] Wenliang Sun,[2] and Chunge Li[6]

[1]*Xuzhou Cumt Backfill Technology Co., Ltd, Xuzhou Jiangsu 221116, China*
[2]*Huaneng Lingtai Shaozhai Coal Industry Co., Ltd, Pingliang, Gansu 272000, China*
[3]*School of Mines, China University of Mining and Technology, Xuzhou, Jiangsu 221116, China*
[4]*Key Laboratory of Deep Coal Resource Mining of the Ministry of Education, China University of Mining and Technology, Xuzhou, Jiangsu 221116, China*
[5]*Honghui No.1 Coal Mine of Gansu Jingyuan Coal Industry and Electricity Power Co., Ltd, Baiyin, Gansu 273000, China*
[6]*Xinjiang Institute of Engineering, Urumqi, Xinjiang 830000, China*

Correspondence should be addressed to Xiaofang Wo; ts21020053a31tm@cumt.edu.cn

Received 13 January 2022; Revised 13 March 2022; Accepted 29 March 2022; Published 16 April 2022

Academic Editor: Lei Wang

Aiming at the serious deformation and failure of mining roadway under the condition of high secondary stress in Xuchang Coal Mine, Shandong Province, the deformation law of surrounding rock under the influence of high secondary stress in the original support belt transport roadway was analyzed by the method of field measurement and numerical simulation, and the control scheme of surrounding rock was put forward. According to the actual site conditions of 3318 working face belt transport drift in Xuchang Coal Mine, this paper proposed a new bolt-net support technology scheme with high strength, high stiffness, and asymmetric characteristics and obtained through numerical simulation analysis: (1) when the 3318 working face begins to mining, the distribution of the maximum principal stress in the surrounding rock of the roadway changes from weak symmetry to strong asymmetry, especially the maximum principal stress in the surrounding rock of the two sides; (2) the superposition effect of leading abutment pressure, lateral abutment pressure, and fault structure has a strong influence on the distribution of the maximum principal stress of roadway surrounding rock. The field industrial test shows that the deformation of the surrounding rock at different parts of the belt transport roadway is significantly reduced after the implementation of the double-height asymmetric bolting support. Among them, the deformation of the roof decreases from 630 mm to 185 mm, the deformation of the left wall decreases from 550~620 mm to 150~170 mm, and the deformation of the right wall decreases from 600 mm to less than 180 mm. The nonuniform deformation degree of the top side is within 1~1.13, indicating that the anchor mesh composite bearing structure is uniformly deformed as a whole, and the overall bearing capacity of the structure is realized.

1. Introduction

After long-term mining, some coal mines in China have entered the middle and later stage of mine life cycle, mining areas with simple occurrence conditions are basically completed, and most of the remaining mining areas are mining areas with strong geological structure influence, the occurrence conditions of coal seams are complex, and geological structures such as faults are developed [1–5]. For this part of the mine, the coal roadway is strongly affected by the fault geological structure, and its surrounding rock maintenance is difficult, so it is always in a difficult situation of repeated repair [6–10]. Because most of the working face is surrounded by existing goaf, the roadway of the working face is always within the strong influence range of the lateral bearing pressure of the goaf [11]. Under the superposition influence of the geological structure and the fixed supporting pressure of the adjacent working face, the roadway has been

repaired many times before the working face is mined and has always been subject to the long-term effect of secondary high stress caused by multiple disturbances [12–16]; when the working face is mined, the mining roadway within a certain range ahead of the working face will have strong deformation.

Aiming at the problem of large deformation of surrounding rock caused by repeated disturbance of deep buried soft rock roadway, some scholars have constructed the stress coupling numerical model of roadway excavation stress field and working face mining stress field, the research shows that the increase or decrease of stress caused by adjacent coal seam mining is less than 15%, and the simple stress change will not lead to the overall failure of roadway support or large deformation of surrounding rock; after repeated disturbance, the mechanical properties of roadway surrounding rock are significantly reduced, which makes it develop from elastic-plastic deformation to loose deformation [17–20]; in view of the serious deformation and damage of the mining roadway under the influence of multiple mining in the close coal seam, taking Cuijiazhai coal mine as a typical case, some scholars analyzed the reasonable position of the mining roadway under the influence of mining and determined that the relative horizontal distance between the mining roadway and the residual coal pillar in the upper coal seam should be greater than 25 m, and the width of the roadway pillar in the working face should be 20 m; the technical scheme of bolt-net cable combined support is put forward [21, 22]; some scholars take the 11271 haulage roadway of Zhaogu No. 1 coal mine as an example; aiming at the problem of large deformation of the roadway under the influence of high stress, weak surrounding rock, and strong mining, scholars analyze and conclude that the main reason for large deformation and failure of surrounding rock of 11271 haulage roadway is that the existing support parameters are unreasonable. Based on the principle of high prestress and prestress diffusion guided by the action mechanism of bolt cable coordinated support and strong side support, the original support scheme is optimized [23–27]; in view of the serious problem of surrounding rock fragmentation and deformation caused by multiple mining in the mining roadway with double roadway layout, taking the auxiliary transportation roadway of Dongliang coal industry 3101 face as an example, some scholars analyzed the direct inducement leading to the destruction of surrounding rock and put forward the "three high" strengthening surrounding rock control technology based on the full section high-strength lengthened anchor rod of roadway+high-strength prestressed anchor cable+high-strength anchor mesh [28–30]. In view of the influence of fault structure on the original rock stress of transportation roadway in working face, some scholars take 3318 working face of Xuchang Coal Mine as an example, analyze and obtain the roadway stress distribution law under the superposition of goaf lateral abutment pressure, adjacent working face abutment pressure, and fault structure, and reveal the stability characteristics of roadway surrounding rock under the action of multiple perturbation stresses [31]. Although Chinese scholars have done a lot of theoretical and practical research on this type of subject, many different factors lead to the deformation of surrounding rock of this kind of mine roadway, so we still need to do a lot of research and exploration [32–36].

By carrying out the technical problems of roadway surrounding rock support under the superposition effect of multiple factors such as fault structure, goaf lateral supporting pressure, and advanced mining stress in this working face, this paper is aimed at deeply analyzing the surrounding rock stability characteristics of this kind of roadway, revealing its surrounding rock failure mechanism, guiding the bolt mesh support design and optimization of this kind of roadway, achieving the ultimate goal of no expansion, and repairing during the roadway service period [37–41]. This study has theoretical and practical significance for maintaining the safety of roadway surrounding rock.

2. Project Overview

Xuchang Coal Mine is one of the main production mines of Shandong Energy Zibo Mining Group. It is located in the northeast of Jining City. The roadway is arranged in the coal seam and excavated along the coal seam floor. The relative ground elevation within the roadway excavation range is about +40 m, the underground elevation is about -320 m, and the maximum buried depth of the roadway is about 360 m. The belt transport roadway of 3318 working face adopts a rectangular section, the net section area of the roadway is 14.88 m^2, the net width is 4800 mm, and the net height is 3100 mm. The direct roof of the coal seam is medium-grained sandstone, with a thickness of 7.80~9.15 m, with an average of 8.98 m; the basic roof is siltstone, with a thickness of 1.60~9.97 m, with an average of 8.36 m; the immediate floor is mudstone, with a thickness of 0~2.8 m, with an average of 0.52 m; the hard floor is siltstone with a thickness of 0~2.75 m and an average of 1.54 m. The engineering background of Xuzhuang Coal Mine is shown in Figure 1.

At present, Xuchang Coal Mine has entered the middle and later stage of the mine life cycle. The mining in the mining areas with simple occurrence conditions is basically completed. Most of the remaining mining areas are mining areas with strong influence of geological structure, with complex occurrence conditions of coal seams and developed geological structures such as faults [31]. Working face 3318 is located between Huangqiao East fault and Huangqiao fault. The length of working face changes with the distance between the two faults, that is, the length of working face gradually decreases from about 128 M at the initial mining to about 40 m at the end of mining. For the belt transport roadway of 3318 working face, the Huangqiao fault structure with an inclination of 70° and a drop of more than 22 m has the strongest influence on it; in addition, DF44 and DF48 faults will be crossed during the excavation of belt transport roadway. The north side of the belt transport roadway of 3318 working face is the goaf of 3302 upper working face, the horizontal distance is about 60 m, and the Huangqiao East fault is between the two working faces. The spatial position relationship between 3318 working face and adjacent working face and fault is shown in Figure 2.

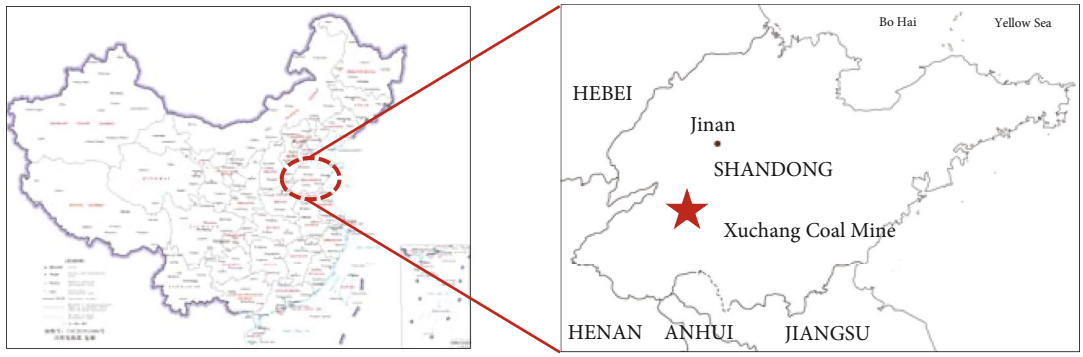

Figure 1: Project background.

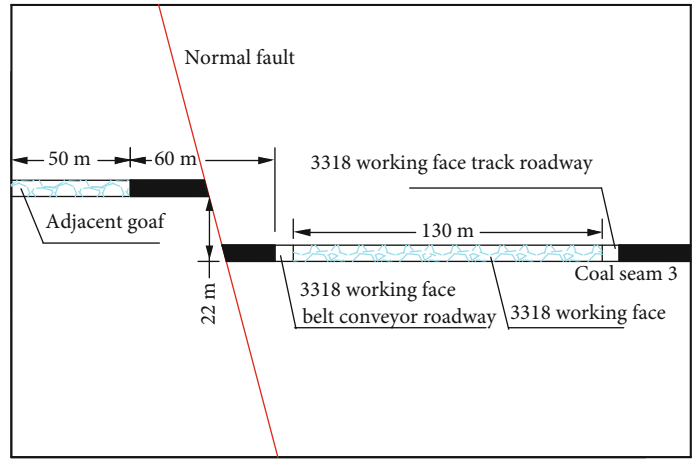

Figure 2: Section of spatial position relationship of 3318 working face.

3. Analysis on Deformation Characteristics of Original Supporting Roadway

In order to analyze the surrounding rock deformation law of the secondary high-stress roadway with multiple disturbances in the haulage roadway of working face 3318 of Xuchang Coal Mine, three measuring stations No. 1, No. 2, and No. 3 are arranged in the 3318 belt transport roadway on site, about 200 m, 600 m, and 1000 m away from the setup room, respectively. 16 surrounding rock deformation measuring points are uniformly arranged clockwise from the bottom corner of the left wall of each measuring station section; 1#, 5#, 9#, and 13# measuring points are located at the lower left, upper left, upper right, and lower right corners of the roadway section, respectively; 2#, 3#, and 4# measuring points are located in the left wall of the roadway; 6#, 7#, and 8# measuring points are located in the roadway roof; 8#, 9#, and 10# measuring points are located in the right wall of the roadway; and 14#, 15#, and 16# measuring points are located in the roadway floor. The surrounding rock deformation of the haulage roadway before and after mining is observed through the section measuring points of each measuring station. The roadway surface deformation and nonuniform deformation of each measuring point of the 1# measuring station section of the haulage roadway before and after mining of 3318 working face are shown in Figures 3 and 4. The nonuniform deformation degree of different parts in a certain section of the roadway is defined as the ratio of the deformation amount of other parts to the deformation amount of this part based on the minimum deformation amount of a certain part of a certain section of the roadway [42, 43]. This value can directly indicate the relative deformation state of roof, slope, and floor surrounding rock.

As shown in Figure 3, when 3318 working face has not been mined, the haulage roadway is affected by the superposition of the lateral bearing pressure and fault structure of the adjacent goaf, and the surrounding rock of the left wall and roof of the roadway is subjected to strong concentrated stress, resulting in a large surface deformation of each measuring point of the left wall and roof relative to the right wall and floor. The deformation of left wall 2#, 3#, and 4# measuring points and side foot 1# measuring points of the roadway is more than 290 mm, and the nonuniform deformation degree is about 14.5; the deformation of the roof 5#, 6#, and 7# three measuring points is more than 355 mm, and the nonuniform deformation reaches 17.75. Compared with the roof and the left wall, the deformation of the right wall 11#, 12#, and 13# measuring points is obviously smaller, and the deformation is between 95 mm and 140 mm; the deformation of the surrounding rock of the roadway floor is small, especially in the middle of the floor. The

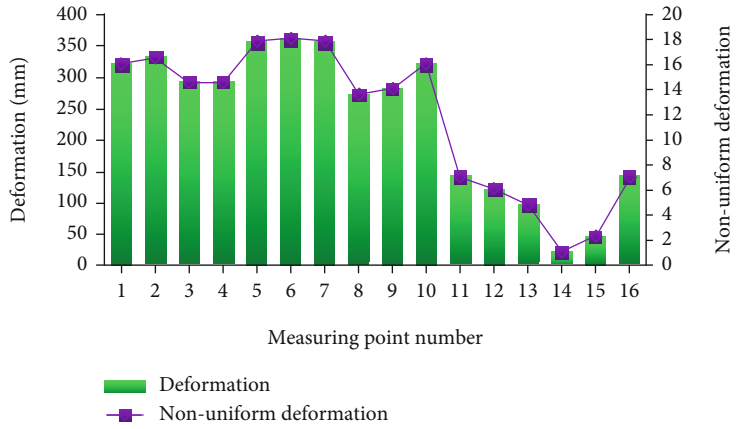

Figure 3: Deformation and nonuniform deformation of each measuring point on the section of haulage roadway 1# measuring station when 3318 working face is not mined.

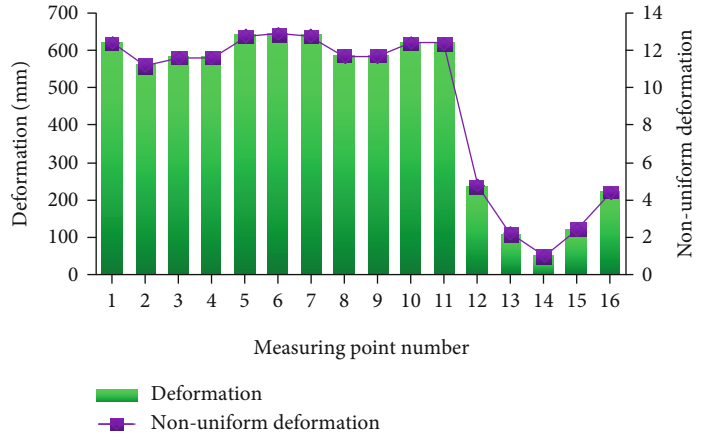

Figure 4: Deformation and nonuniform deformation of each measuring point on the section of the haulage roadway 1# measuring station after mining in 3318 working face.

deformation is the minimum value of 20 mm at all monitoring points of the section of the station. Therefore, the deformation at this point is taken as the reference value of the nonuniform deformation of the surrounding rock. It can be seen that when the haulage roadway is not affected by the advance bearing pressure of 3318 working face, the action positions of asymmetric support are top middle, left wall middle, left wall foot, and right wall top in turn.

As shown in Figure 4, when the 3318 working face starts mining, after the haulage roadway is affected by the lateral bearing pressure of the adjacent goaf, the influence of fault structure, and the multiple overlapping influence of the advance bearing pressure of the working face, the deformation increase of surrounding rock in different parts of the roadway reaches more than 50%, especially the surrounding rock of the roadway roof, the left wall, and the right wall, including the middle 6#. The deformation of surrounding rock at 7# and 8# measuring points increases to more than 585 mm, and the deformation of left 1#, 2#, 3#, and 4# measuring points, right middle 10#, 11# measuring points, and roof 9# measuring points are all more than 560 mm. Compared with the top side, the deformation of the floor is small. The middle position of the floor is the minimum value of the section deformation of the station, and this value is the benchmark value of the nonuniform deformation of surrounding rock. It can be seen that when the haulage roadway is subjected to the advance bearing pressure of 3318 working face, the action positions of asymmetric support are top middle, left wall middle, left wall foot, and right wall top in turn.

4. Simulation of Stress Distribution Law of Surrounding Rock of Multidisturbed Secondary High-Stress Roadway

4.1. Construction of Numerical Simulation Model. In order to analyze the stress distribution and evolution law of surrounding rock of haulage roadway under the superposition effect of lateral bearing pressure in adjacent goaf, fault structure, and advance bearing pressure in 3318 working face, the three-dimensional numerical analysis model established by using FLAC3D numerical analysis software is shown in Figure 5, which comprehensively reflects the superposition

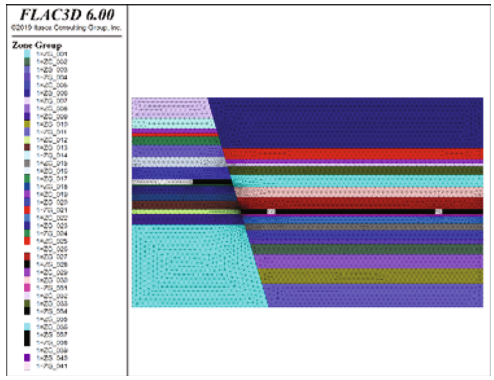

Figure 5: Numerical simulation model.

effect of fault structure and lateral bearing pressure of adjacent goaf [44–46]. The physical and mechanical parameters of coal and rock strata referenced by the model are shown in Table 1. The length × width × height of the numerical model is 300 m × 200 m × 200 m, respectively. 3318 working face and its mining roadway are located in the middle of the model, in which the horizontal distance between the haulage roadway and the fault is 20 m, and the horizontal distance between the haulage roadway and the edge of the adjacent goaf is 60 m; at the same time, the adjacent working face is modeled by the semi-infinite mining method, that is, the adjacent goaf is located at the left boundary of the model. In the model, the mesh stress and deformation iteration adopt the Mohr-Coulomb strength criterion, that is, the failure surface shear stress criterion. In addition, the front, rear, left, and right boundaries of the model are support boundary conditions, the bottom boundary is fixed boundary conditions, and the upper boundary is stress boundary conditions. A uniformly distributed load of 6.5 MPa is applied on the upper part to simulate the self-weight of the 360 m thick rock layer on the model. Due to the development of joints and fissures in the rock mass near the coal seam and serious water deliquescence and weathering, the physical and mechanical parameters of the direct top and bottom strata of the coal seam are slightly weakened. The interface command is used to simulate the fault in the model. The mechanical parameters of the fault contact surface are shear stiffness 200 GPa, normal stiffness 200 GPa, internal friction angle 15°, and cohesion 0.4 MPa, and the sliding mode is opened at the same time. In order to analyze the influence of fault structure and lateral bearing pressure of adjacent goaf on the original rock stress at the roadway position, monitoring points are set at the section center of the haulage roadway of 3318 working face to monitor the evolution law of disturbed secondary stress field formed by the superposition effect of fault structure, lateral bearing pressure of goaf, and advance mining stress of this working face in real time.

4.2. Analysis of Numerical Simulation Results. Through numerical simulation, the vertical stress distribution law of roadway surrounding rock under the superposition effect of multiple factors such as fault structure, goaf lateral bearing pressure, and advance mining stress of the working face is analyzed, as shown in Figure 6, the peak value of superimposed bearing pressure appears at 10 m of the advance working face. Therefore, this paper mainly analyzes the stress distribution law of roadway surrounding rock around the peak value of superimposed bearing pressure. In the mining process of 3318 working face, the roof strata gradually bend and sink, the load of the overlying strata is transferred to the surrounding rock of the mining roadway, and a semicircular concentrated stress area is formed in the surrounding rock of the two sides of the roadway, which presents asymmetric characteristics.

The peak value of concentrated stress in the surrounding rock of the right wall of the roadway reaches 22.3 MPa, the stress concentration factor reaches about 2.5, and the peak position is 5.5 m away from the surface of the surrounding rock of the right wall; in contrast, the stress concentration degree of the surrounding rock of the left wall is slightly small, but the peak value of the concentrated stress still reaches about 21 MPa and appears 4.5 m away from the surface of the surrounding rock of the left wall. In addition, the stress reduction areas of surrounding rock in the roof and floor of the roadway are large, which are 4 m and 3.8 m, respectively, and the stress drops significantly in the range of 0~3 m of the roof and floor, and their values are below 2 MPa. Compared with the stress distribution law of roadway surrounding rock under the condition of no mining in working face 3318, the concentrated stress range of the two sides of the roadway is significantly developed, especially the surrounding rock of the right wall. The peak value of concentrated stress increases sharply from 14.6 MPa to more than 22 MPa. Moreover, the strongly affected area of concentrated stress develops from a circular area with a radius of about 3 m to a semicircular area with a radius of about 20 m (approximately circular arc distribution in the section shown in the figure), resulting in the strong superposition of lateral bearing pressure and advance bearing pressure on the surrounding rock of the right wall, accelerating the failure and instability of rock mass after the peak; at the same time, the peak value of concentrated stress in the surrounding rock of the left wall also increased significantly, from 14.9 MPa to about 21 MPa, and the distribution range of concentrated stress and the action area of stress peak expanded from a circular area with a diameter of about 4 m to a semicircular area with a diameter of about 18 m, and the action range of high concentrated stress expanded rapidly. In order to further analyze the asymmetric characteristics of the surrounding rock stability of the haulage roadway in working face 3318, the distribution law of the maximum principal stress in the surrounding rock of the roadway is analyzed in detail, and its distribution law is shown in Figures 7 and 8.

As shown in Figure 7, when working face 3318 has not been mined, the maximum principal stress of roadway surrounding rock is mainly affected by the superposition of lateral bearing pressure and fault structure in the goaf adjacent to working face 3302, and its maximum principal stress presents a weak symmetrical distribution. The reduction range of the maximum principal stress on the left wall of the roadway is the smallest, about 0.5 m, but the maximum principal

Table 1: Physical and mechanical parameters of coal and rock stratum.

Number	Rock lithology	Thickness (m)	Density ($kg \cdot m^3$)	Bulk modulus (GPa)	Shear modulus (GPa)	Friction angle (°)	Cohesion (MPa)	Tensile strength (MPa)
1	Loess	34	1960	0.25	0.09	25	8.5	0.35
2	Fine-grained sandstone	7	2610	2.23	1.67	38	3	3.15
3	Mudstone	3	2604	5.88	3.19	41	5.4	3.18
4	Siltstone	2	2603	7	4	43	6.3	4.99
5	Medium-grained sandstone	6	2987	4.34	2.3	40	4.3	2.7
6	Fine-grained sandstone	8	2690	2.23	1.67	32	3.8	3.17
7	Siltstone	7	2558	6.32	3.61	33	8.7	3.07
8	Medium-grained sandstone	8	2987	4.34	2.3	40	4.3	2.07
9	Coal	4	1445	0.71	0.49	22	2.44	0.24
10	Mudstone	1.5	2604	5.88	3.19	41	5.4	3.18
11	Siltstone	5	2603	7	4	43	6.3	4.99
12	Medium-grained sandstone	5	2987	4.34	2.3	40	4.3	2.7
13	Fine-grained sandstone	6	2690	2.23	1.67	32	3.8	3.17
14	Mudstone	3	2604	5.88	3.19	41	5.4	3.18
15	Siltstone	7	2558	6.32	3.61	33	8.7	3.07
16	Fine-grained sandstone	10	2610	2.23	1.67	38	3	3.15
17	Medium-grained sandstone	10	2987	4.34	2.3	40	4.3	2.7
18	Siltstone	16	2603	7	4	43	6.3	4.99

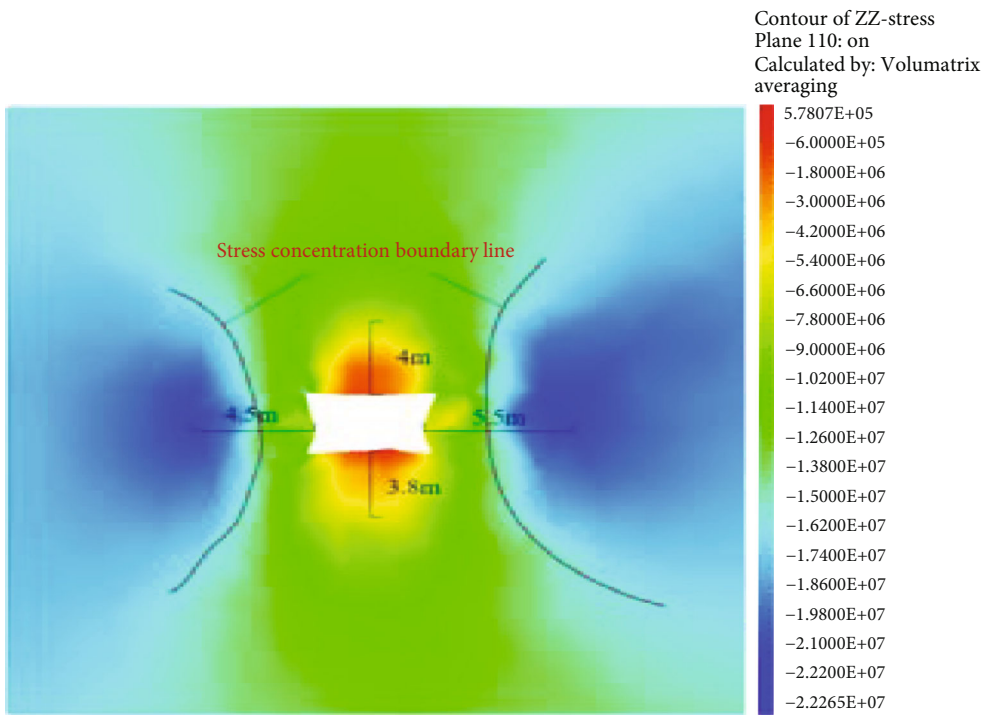

Figure 6: Vertical stress distribution law of surrounding rock of multidisturbance secondary high-stress roadway.

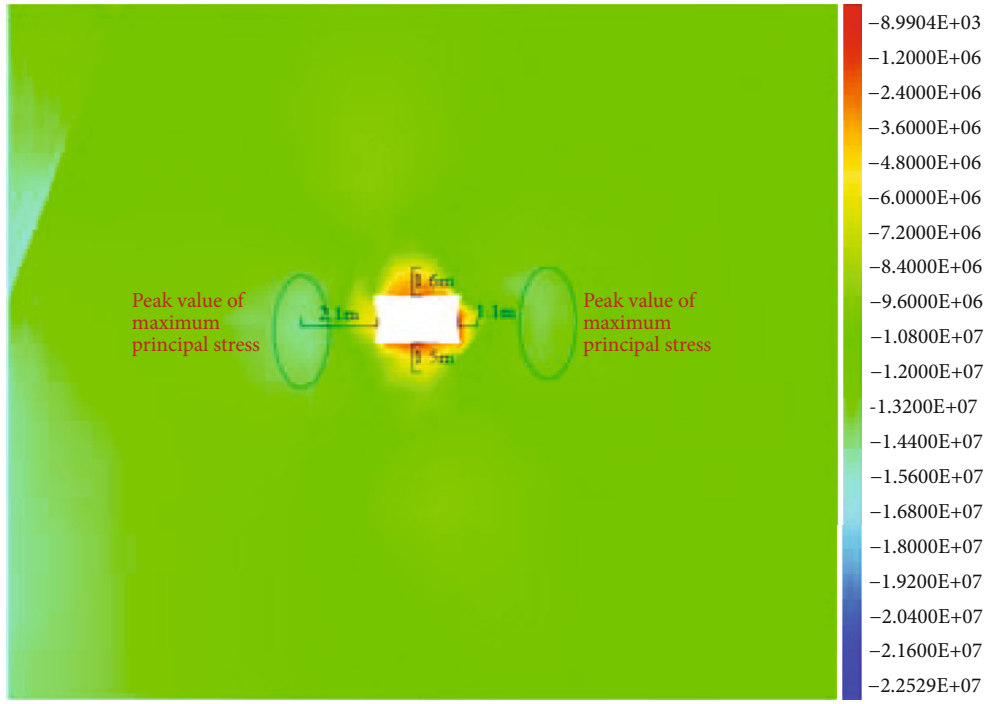

Figure 7: Distribution law of maximum principal stress of roadway surrounding rock under the condition of no mining in 3318 working face.

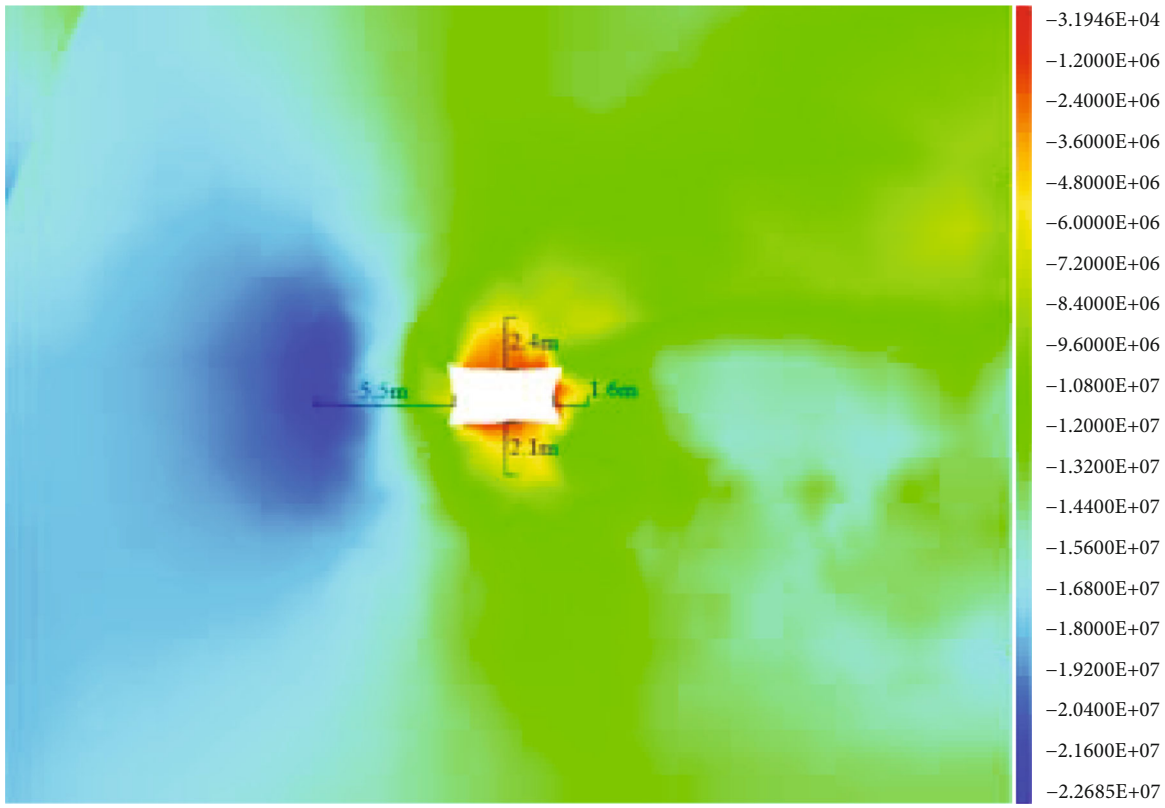

Figure 8: Distribution characteristics of maximum principal stress of surrounding rock of multidisturbance secondary high-stress haulage roadway.

stress peak appears at 2.1 m from the surrounding rock surface; secondly, the reduction range of surrounding rock stress on the surface of roadway roof and floor is relatively consistent, which is about 1.5 m; the stress reduction range of surrounding rock on the surface of the right wall is relatively large compared with that of the left wall, reaching

more than 1.1 m, but the maximum principal stress peak appears at 2 m away from the surrounding rock surface, which is similar to the maximum principal stress peak of the left wall. As shown in Figure 8, in the mining process of working face 3318, the maximum principal stress in the surrounding rock of the haulage roadway shows a significant asymmetric distribution law, and the direction of the maximum principal stress is distributed along the tangential direction of the roadway section. The maximum principal stress at the position 5.5 m away from the left wall rock surface has a significant concentration effect, and the peak value of the maximum principal stress is 22.1 MPa; on the contrary, there is no significant concentration in the surrounding rock of the right wall, roof, and floor of the roadway, but mainly the drop of the maximum principal stress of the surrounding rock on the roadway surface. The stress reduction area of the roof rock mass reaches 2.4 m, which is relatively large compared with other locations, followed by the floor stress reduction area, but it still reaches about 2.1 m, and the stress reduction range of the right wall is relatively small, reaching 1.6 m.

By comparing and analyzing Figures 7 and 8, it can be seen that after the mining of working face 3318 begins, the distribution law of the maximum principal stress of the surrounding rock of the roadway changes from weak symmetry to strong asymmetry, especially the maximum principal stress in the surrounding rock of the two sides. The results show that the superposition effect of advance bearing pressure, lateral bearing pressure, and fault structure has a strong impact on the distribution law of the maximum principal stress of roadway surrounding rock, which is as follows: (1) the concentration of the maximum principal stress of the surrounding rock of the left wall is significant, and the action area of the stress peak and the strong influence range of the maximum principal stress increase sharply; (2) the variation of the maximum principal stress concentration on the right wall is slightly small, but the stress reduction range increases significantly; (3) there is no maximum principal stress concentration in the surrounding rock of roof and floor, but the stress reduction area of surface surrounding rock develops rapidly. The above characteristics show that the superposition effect of the advance bearing pressure produced by the mining of 3318 working face, the lateral bearing pressure of goaf, and fault structure is significant, which makes the rock mass on the roadway surface in a typical unidirectional stress state, especially the concentrated stress on the left wall, accelerates the shear deformation and fracture surface development in the surrounding rock, and leads to the asymmetric instability of the surrounding rock.

5. Optimization Design of Roadway Support Parameters

In the mining process of 3318 working face, the belt transport roadway is in the secondary high-stress field after multiple disturbances, which belongs to a typical complex high-stress roadway. Therefore, according to the surrounding rock stress environment and surrounding rock conditions of belt transport roadway, combined with field measurement and numerical simulation analysis, and based on the advanced optimization idea and optimal guiding parameters of bolt mesh support parameters of complex high-stress roadway in Xuchang Coal Mine, a new bolt mesh support technical scheme with high strength, high stiffness, and asymmetric characteristics suitable for belt transport roadway in 3318 working face of Xuchang Coal Mine is proposed. In the technical scheme, two support sections A and B of 3318 working face are arranged alternately, with a row spacing of 800 mm, as shown in Figure 9.

(1) Support parameters of section A: adopted for roadway side $\Phi 18 \times 2400$ mm 20MnSi high-strength full thread steel anchor bolts with spacing of 850 mm are lengthened and anchored with one CK2350 (end) and one K2350 resin anchoring agent, respectively; at the same time, the specification is a 2800 $\times$ 80 mm special-shaped steel belt that connects adjacent anchor bolts in section A. Roof anchor cable $\Phi 21.6 \times 7000$ mm 1860 steel strand is supported with a spacing of 1000 mm. One CK2350 (end) and two K2350 resin anchoring agents are used for lengthening and anchoring, respectively. Meanwhile, the specification is a $4600 \times 280 \times 3$ mm W-shaped steel belt that connects adjacent anchor cables in section A

(2) Support parameters of section B: roof anchor cable $\Phi 17.8 \times 4000$ mm 1860 steel strand is supported with a spacing of 1000 mm. One CK2350 (end) and two K2350 resin anchoring agents are used for lengthening and anchoring, respectively; the adopted specification is a $4600 \times 280 \times 3$ mm W-shaped steel belt that connects adjacent anchor cables in section A. The upper part of one side of the working face adopts the joint arrangement of the anchor bolt and anchor cable, with a spacing of 850 mm. External binding arrangement of top and bottom $\Phi 18 \times$ 2400 mm 20MnSi high-strength full thread steel bolt support, used in the upper $\Phi 17.8 \times 4000$ mm 1860 steel strand support. One CK2350 (end) and one K2350 resin anchoring agent are used for lengthening and anchoring of anchor bolts; one CK2350 (end) and two K2350 resin anchoring agents are used for lengthening and anchoring of anchor cables; the adopted specification is a 2800×80 mm special-shaped steel belt that connects adjacent anchor bolts and anchor cables in section A. The slope on one side of the fault adopts $\Phi 18 \times 2400$ mm 20MnSi high-strength full-thread steel anchor bolt with a spacing of 850 mm. One CK2350 (end) and one K2350 resin anchoring agent are used for lengthening anchoring, respectively. The adopted specification is a 2800×80 mm special-shaped steel belt that connects adjacent anchor bolts in section A

(3) Parameters of reinforced support at the side of the fault: "Wuhua" 1860 steel strands with $\Phi 17.8 \times$ 4000 mm are arranged, the spacing is 1700 mm, and the row spacing is 1600 mm. A CK2350 (end) and two K2350 resin anchoring agents are used for

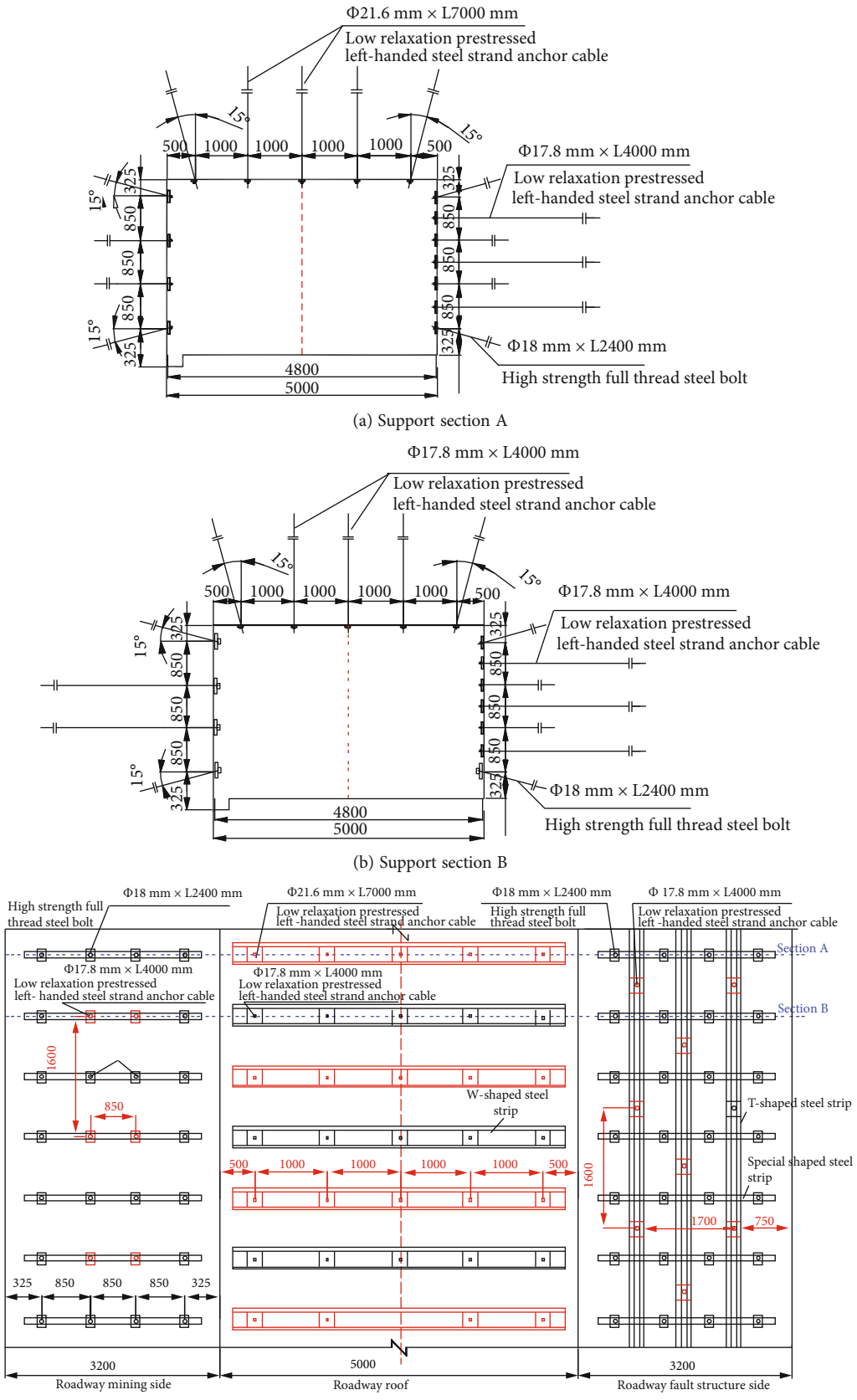

Figure 9: Schematic diagram of optimized support of 3318 belt transport roadway (unit: mm).

extension anchoring. A 1800 mm long T-shaped steel belt is arranged along the axial direction of the roadway to connect the adjacent reinforcing anchor cable. There is an overlapping relationship between the adjacent steel belts along the axial direction of the roadway, and the overlapping length is 100 mm. The anchor cable is used to compress the overlapping part

The supporting cast steel nuts shall be used to apply pretightening force to the anchor bolts, and the pretightening torque shall not be less than 300 N·m; the specification of the anchor pallet is an arc-shaped steel pallet of 120 × 120 × 10 mm; the anchor cables shall be pretensioned with supporting two core locks, and the pretightening force shall not be less than 100 kN or the pressure indication of tensioning jack shall not be less than 25 MPa. The mesh made of 10# iron wire is 50 × 50 mm diamond metal mesh that supports the roadway side, and the specification of roof metal mesh is 5200 × 1100 mm. The specification of two sides is 2600 × 2000 mm diamond metal mesh that shall be used for longitudinal overlapping. Single strand 10# iron wire shall be used for connection between top nets, side nets, and top and side nets at a spacing of 200 mm, and the overlapping shall not be less than 100 mm.

6. Field Application Effect Analysis

In order to reasonably evaluate the surrounding rock control effect of high-strength and high-stiffness asymmetric bolt mesh support technology scheme for multidisturbance secondary high-stress roadway, after the new support scheme is adopted, No. 3 observation station is arranged in the belt transport roadway of 3318 working face to measure the surrounding rock deformation of each measurement point in the section of the observation station during the mining process of the working face. By means of field observation, we can see the deformation characteristics of surrounding rock of double-height asymmetric bolt mesh support roadway.

After the implementation of double-height asymmetric anchor mesh support in the roadway, the deformation of surrounding rock in different parts of the roadway is significantly reduced in the mining process of working face 3318, the deformation of surrounding rock in different parts of the roadway is significantly reduced, the deformation of roof is reduced from more than 630 mm to about 185 mm, the deformation of surrounding rock in the left wall is reduced from 550~620 mm to 150~170 mm, and the deformation of surrounding rock in the right wall is reduced from 600 mm to less than 180 mm. If the central deformation of the floor is taken as the benchmark of the nonuniform deformation of the surrounding rock, when the double-height asymmetric anchor mesh support is not adopted, the nonuniform deformation of the middle of the roof, the left wall foot, the right wall foot, and the right wall foot is the largest, reaching between 11 and 12, belonging to the area of strong nonuniform deformation; after the new anchor mesh support is adopted, the nonuniform deformation of the top side is significantly reduced by more than 50%, which is basically stable within 6~6.5. For the composite structure formed by the anchor mesh support and surrounding rock at the top, the deformation of the surrounding rock at the top of the left side is taken as the benchmark of the nonuniform deformation of the bearing structure. After adopting the double-height asymmetric anchor mesh support scheme, the nonuniform deformation of the top side is within 1~1.13. This phenomenon shows that the anchor net composite bearing structure has uniform deformation and realizes the overall bearing of the structure.

7. Conclusion

(1) Due to the superposition of advance bearing pressure, lateral bearing pressure, and fault tectonic stress, the stress of roadway surrounding rock shows high asymmetry

(2) A new bolt mesh support technology scheme with high strength, high stiffness, and asymmetric characteristics suitable for the belt transportation roadway of 3318 working face in Xuchang Coal Mine is put forward

(3) The field industrial test shows that after the implementation of double-height asymmetric anchor mesh support, the deformation of surrounding rock in different parts of the roadway is significantly reduced. The roof deformation is reduced from more than 630 mm to about 185 mm, the surrounding rock deformation of the left wall is reduced from 550~620 mm to 150~170 mm, the surrounding rock deformation of the right wall is reduced from 600 mm to less than 180 mm, and the nonuniform deformation of the top side is within 1~1.13. It shows that the anchor net composite bearing structure has uniform deformation and realizes the overall bearing of the structure

Data Availability

The Microsoft Excel Worksheet data used to support the findings of this study are available from the corresponding author upon request.

Conflicts of Interest

The authors declare that they have no competing interests.

Acknowledgments

This research was funded by the projects of "the Fundamental Research Funds for the Central Universities (2020ZDPY0221 and 2021QN1003)", the "National Natural Science Foundation of China (52104106 and 52174089)", and the "Basic Research Program of Xuzhou (KC21017)."

References

[1] H. Lin and B. Zhang, "Study of soft rock roadway support technique," in *1st International Symposium on Mine Safety Science and Engineering (ISMSSE)*, vol. 26, pp. 321–326, Beijing, PEOPLES R CHINA, 2011.

[2] Q. Liu, J. Li, and B. Liu, "The stability control theory of deep coal mine roadway," *Energy Education Science and Technology Part a-Energy Science and Research*, vol. 30, no. 1, pp. 521–528, 2012.

[3] S. G. Liu, J. B. A. Bai, X. Y. Wang, S. Yan, and J. X. Zhao, "Field and numerical study on deformation and failure characteristics of deep high-stress main roadway in Dongpang coal mine," *Sustainability*, vol. 13, no. 15, p. 8507, 2021.

[4] B. T. Shen, "Coal mine roadway stability in soft rock: a case study," *Rock Mechanics and Rock Engineering*, vol. 47, no. 6, pp. 2225–2238, 2014.

[5] X. J. Yang, E. Y. Wang, Y. J. Wang, Y. B. Gao, and P. Wang, "A study of the large deformation mechanism and control techniques for deep soft rock roadways," *Sustainability*, vol. 10, no. 4, p. 1100, 2018.

[6] Y. H. Cheng, F. X. Jiang, and L. H. Kong, "Self-bearing capacity for surrounding rock of composite roof of coal roadways and deformation control in deep high stress mine," in *Proceedings of the ICMHPC-2010 International Conference on Mine Hazards Prevention and Control*, Atlantis Press, p. 415-+, Qingdao, PEOPLES R CHINA, 2010.

[7] J. C. Feng, S. F. Yin, Z. H. Cheng et al., "Deformation and failure mechanism of surrounding rock in mining-influenced roadway and the control technology," *Shock and Vibration*, vol. 2021, Article ID 5588314, 14 pages, 2021.

[8] S. T. Gu, B. Y. Jiang, G. S. Wang, H. B. Dai, and M. P. Zhang, "Occurrence mechanism of roof-fall accidents in large-section coal seam roadways and related support design for Bayangaole coal mine, China," *Advances in Civil Engineering*, vol. 2018, Article ID 6831731, 17 pages, 2018.

[9] Q. S. Wu, P. Kong, Q. L. Wu, X. G. Xu, X. Y. Wu, and T. Guo, "Study on overburden rock movement and stress distribution characteristics under the influence of a normal fault," *Advances in Civil Engineering*, vol. 2020, Article ID 7859148, 16 pages, 2020.

[10] Y. T. Sun, G. C. Li, N. Zhang, Q. L. Chang, J. H. Xu, and J. F. Zhang, "Development of ensemble learning models to evaluate the strength of coal-grout materials," *International Journal of Mining Science and Technology*, vol. 31, no. 2, pp. 153–162, 2021.

[11] C. Li, Z. Wu, W. L. Zhang, Y. H. Sun, C. Zhu, and X. H. Zhang, "A case study on asymmetric deformation mechanism of the reserved roadway under mining influences and its control techniques," *Geomechanics and Engineering*, vol. 22, no. 5, pp. 449–460, 2020.

[12] S. C. Li, Q. Wang, H. T. Wang et al., "Model test study on surrounding rock deformation and failure mechanisms of deep roadways with thick top coal," *Tunnelling and Underground Space Technology*, vol. 47, pp. 52–63, 2015.

[13] Y. W. Gao, C. Wang, Y. Liu, Y. Y. Wang, and L. C. Han, "Deformation mechanism and surrounding rock control in high-stress soft rock roadway: a case study," *Advances in Civil Engineering*, vol. 2021, Article ID 9950391, 15 pages, 2021.

[14] Y. T. Sun, R. Y. Bi, Q. L. Chang et al., "Stability analysis of roadway groups under multi-mining disturbances," *Applied Sciences*, vol. 11, no. 17, p. 7953, 2021.

[15] C. X. Zhao, Y. M. Li, G. Liu, and X. R. Meng, "Mechanism analysis and control technology of surrounding rock failure in deep soft rock roadway," *Engineering Failure Analysis*, vol. 115, p. 104611, 2020.

[16] W. Zhang, Z. M. He, D. S. Zhang, D. H. Qi, and W. S. Zhang, "Surrounding rock deformation control of asymmetrical roadway in deep three-soft coal seam: a case study," *Journal of Geophysics and Engineering*, vol. 15, no. 5, pp. 1917–1928, 2018.

[17] J. C. Chang, K. He, Z. Q. Yin, W. F. Li, S. H. Li, and D. D. Pang, "Study on the instability characteristics and bolt support in deep mining roadways based on the surrounding rock stability index: example of Pansan coal mine," *Advances in Civil Engineering*, vol. 2020, Article ID 8855335, 16 pages, 2020.

[18] Q. Wang, R. Pan, B. Jiang et al., "Study on failure mechanism of roadway with soft rock in deep coal mine and confined concrete support system," *Engineering Failure Analysis*, vol. 81, pp. 155–177, 2017.

[19] H. L. Zhang, J. B. Jiao, and L. G. Wang, "Yield evolution mechanism and control technology of roadway surrounding rock in deep mine," in *2nd international conference on electronic and mechanical engineering and information technology (EMEIT)*, vol. 23, Shenyang, PEOPLES R CHINA, 2012Atlantis Press.

[20] Y. T. Sun, G. C. Li, J. F. Zhang, J. B. Sun, J. D. Huang, and R. Taherdangkoo, "New insights of grouting in coal mass: from small-scale experiments to microstructures," *Sustainability*, vol. 13, no. 16, p. 9315, 2021.

[21] J. C. Chang, D. Li, T. F. Xie, W. B. Shi, and K. He, "Deformation and failure characteristics and control technology of roadway surrounding rock in deep coal mines," *Geofluids*, vol. 2020, Article ID 8834347, 15 pages, 2020.

[22] S. Q. Yang, M. Chen, H. W. Jing, K. F. Chen, and B. Meng, "A case study on large deformation failure mechanism of deep soft rock roadway in Xin'An coal mine, China," *Engineering Geology*, vol. 217, pp. 89–101, 2017.

[23] H. Li, W.-J. Liu, and W.-G. Qiao, "Study on high prestressed anchor beam supporting optimization technology in deep roadway," in *3rd International Conference on Civil Engineering, Architecture and Building Materials (CEABM 2013)*, pp. 353–356, Jinan, PEOPLES R CHINA, 2013.

[24] Y. D. Jiang, L. Xiong, W. X. Zhou, X. J. Han, S. X. Mei, and J. Hu, "Research on high ground stress and soft rock roadway supporting technology of Bide coal mine," in *2nd International Conference on Structures and Building Materials (ICSBM)*, pp. 446–449, Trans Tech Publications Ltd, Hangzhou, PEOPLES R CHINA, 2012.

[25] W. S. Xu, W. T. Xu, and Y. H. Cheng, "Research on the reasonable strengthening time and stability of excavation unloading surrounding rock of high-stress rock mass," *Geofluids*, vol. 2021, Article ID 3508661, 13 pages, 2021.

[26] Y. T. Sun, R. Y. Bi, J. B. Sun et al., "Stability of roadway along hard roof goaf by stress relief technique in deep mines: a theoretical, numerical and field study," *Geomechanics and Geophysics for Geo-Energy and Geo-Resources*, vol. 8, no. 2, p. 16, 2022.

[27] C. W. Zang, M. Chen, G. C. Zhang, K. Wang, and D. D. Gu, "Research on the failure process and stability control technology in a deep roadway: numerical simulation and field test," *Energy Science & Engineering*, vol. 8, no. 7, pp. 2297–2310, 2020.

[28] R. Peng, X. R. Meng, G. M. Zhao, Z. H. Ouyang, and Y. M. Li, "Multi-echelon support method to limit asymmetry instability in different lithology roadways under high ground stress,"

Tunnelling and Underground Space Technology, vol. 108, article 103681, 2021.

[29] L. J. Zheng, Y. J. Zuo, Y. F. Hu, and W. Wu, "Deformation mechanism and support technology of deep and high-stress soft rock roadway," *Advances in Civil Engineering,*, vol. 2021, article 6634299, pp. 1–14, 2021.

[30] H. W. Jing, J. Y. Wu, Q. Yin, and K. Wang, "Deformation and failure characteristics of anchorage structure of surrounding rock in deep roadway," *International Journal of Mining Science and Technology*, vol. 30, no. 5, pp. 593–604, 2020.

[31] B. Zhang, H. Q. Zhou, Q. L. Chang, X. Zhao, and Y. T. Sun, "The stability analysis of roadway near faults under complex high stress," *Advances in Civil Engineering,*, vol. 2020, article 8893842, pp. 1–10, 2020.

[32] J. T. Hu, D. G. Lin, and R. M. Zhao, "Stabilization control techniques for a roadway in deep high-stress soft surrounding rock," in *8th Russian-Chinese Symposium on Coal in the 21st Century-Mining, Processing, Safety*, vol. 92, pp. 213–219, Atlantis Press, Kemerovo, RUSSIA, 2016.

[33] C. K. Liu, J. X. Ren, K. Zhang, and S. J. Chen, "Numerical studies on surrounding rock deformation controlled by pressure relief groove in deep roadway," in *International Symposium on Resource Exploration and Environmental Science (REES)*, vol. 64, Ordos, PEOPLES R CHINA, 2017Iop Publishing Ltd.

[34] Z. T. Mao and Y. P. Zhu, "Study of stability assessment method for deep surrounding rock," in *3rd International Conference on Civil, Architectural and Hydraulic Engineering (ICCAHE)*, pp. 565–569, Trans Tech Publications Ltd, Hangzhou, PEOPLES R CHINA, 2014.

[35] G. C. Li, Y. T. Sun, J. F. Zhang et al., "Experiment and application of coalcrete on roadway stability: a comparative analysis," *Advances in Materials Science and Engineering*, vol. 2020, Article ID 6813095, 14 pages, 2020.

[36] Y. Yuan, W. J. Wang, S. Q. Li, and Y. J. Zhu, "Failure mechanism for surrounding rock of deep circular roadway in coal mine based on mining-induced plastic zone," *Advances in Materials Science and Engineering*, vol. 2018, Article ID 1835381, 14 pages, 2018.

[37] Z. C. Qin, B. Cao, Y. L. Liu, and T. Li, "Study on in situ stress measurement and surrounding rock control technology in deep mine," *Geofluids*, vol. 2020, Article ID 8839333, 12 pages, 2020.

[38] M. Su and X. H. Gao, "Research of the surrounding rock deformation control technology in roadway under multiple excavations and mining," *Shock and Vibration*, vol. 2021, Article ID 6681184, 14 pages, 2021.

[39] Y. L. Xu, K. R. Pan, and H. Zhang, "Investigation of key techniques on floor roadway support under the impacts of superimposed mining: theoretical analysis and field study," *Environment and Earth Science*, vol. 78, no. 15, p. 14, 2019.

[40] Z. Z. Xie, N. Zhang, X. W. Feng, D. X. Liang, Q. Wei, and M. Y. Weng, "Investigation on the evolution and control of surrounding rock fracture under different supporting conditions in deep roadway during excavation period," *International Journal of Rock Mechanics and Mining Sciences*, vol. 123, article 104122, 2019.

[41] H. Liu, J. Dai, J. Q. Jiang, P. Wang, and J. Q. Yang, "Analysis of overburden structure and pressure-relief effect of hard roof blasting and cutting," *Advances in Civil Engineering*, vol. 2019, Article ID 1354652, 14 pages, 2019.

[42] H. Q. Yang, N. Zhang, C. L. Han et al., "Stability control of deep coal roadway under the pressure relief effect of adjacent roadway with large deformation: a case study," *Sustainability*, vol. 13, no. 8, p. 4412, 2021.

[43] W. H. Zha and D. F. Wu, "Study on coupling relationship between surrounding rock deformation and support parameters in deep roadway," in *International Conference on Civil, Architecture and Disaster Prevention*, vol. 218, Anhui Jianzhu Univ, Sch Civil Engn, Hefei, PEOPLES R CHINA, 2018Iop Publishing Ltd.

[44] Y. T. Sun, G. C. Li, J. F. Zhang, B. C. Yao, D. Y. Qian, and J. D. Huang, "Numerical investigation on time-dependent deformation in roadway," *Advances in Civil Engineering*, vol. 2021, Article ID 4280139, 7 pages, 2021.

[45] S. Yang, G. C. Li, R. Y. Bi, B. C. Yao, R. G. Feng, and Y. T. Sun, "The stability of roadway groups under rheology coupling mining disturbance," *Sustainability*, vol. 13, no. 21, p. 12300, 2021.

[46] S. Zhang, D. S. Zhang, H. Z. Wang, and S. S. Liang, "Discrete element simulation of the control technology of large section roadway along a fault to drivage under strong mining," *Journal of Geophysics and Engineering*, vol. 15, no. 6, pp. 2642–2657, 2018.